JARO 02: 118–129 (2001)
DOI: 10.1007/s101620010075

JARO
Journal of the Association for Research in Otolaryngology

Spiral Ligament Pathology: A Major Aspect of Age-Related Cochlear Degeneration in C57BL/6 Mice

STEPHANIE HEQUEMBOURG[1] AND M. CHARLES LIBERMAN[1,2]

[1]*Eaton–Peabody Laboratory, Massachusetts Eye and Ear Infirmary, Boston, MA 02114, USA*
[2]*Department of Otology and Laryngology, Harvard Medical School, Boston, MA 02114, USA*

Received: 5 September 2000; Accepted: 2 January 2001; Online publication: 4 May 2001

ABSTRACT

Data from systematic, light microscopic examination of cochlear histopathology in an age-graded series of C57BL/6 mice (1.5–15 months) were compared with threshold elevations (measured by auditory brain stem response) to elucidate the functionally important structural changes underlying age-related hearing loss in this inbred strain. In addition to quantifying the degree and extent of hair cell and neuronal loss, all structures of the cochlear duct were qualitatively evaluated and any degenerative changes were quantified. Hair cell and neuronal loss patterns suggested two degenerative processes. In the basal half of the cochlea, inner and outer hair cell loss proceeded from base to apex with increasing age, and loss of cochlear neurons was consistent with degeneration occurring secondary to inner hair cell loss. In the apical half of the cochlea with advancing age, there was selective loss of outer hair cells which increased from the middle to the extreme apex. A similar gradient of ganglion cell loss was noted, characterized by widespread somatic aggregation and demyelination. In addition to these changes in hair cells and their innervation, there was widespread degeneration of fibrocytes in the spiral ligament, especially among the type IV cell class. The cell loss in the ligament preceded the loss of hair cells and/or neurons in both space and time suggesting that fibrocyte pathology may be a primary cause of the hearing loss and ultimate sensory cell degeneration in this mouse strain.

Keywords: cochlea, hearing, histopathology, aging

Correspondence to: Dr. M. Charles Liberman • Eaton–Peabody Laboratory • Massachusetts Eye and Ear Infirmary • 243 Charles Street, Boston, MA 02114. Telephone: (617) 573-3745; fax: (617) 720-4408; email: mcl@epl.meei.harvard.edu

INTRODUCTION

The C57BL/6 strain of inbred mice has been suggested as a useful animal model of presbycusis, or age-related hearing loss (AHL), seen in human populations (Henry and Chole 1980; Li and Borg 1991). As with human presbycusis, the AHL in C57BL/6 mice begins at the highest test frequencies. As time progresses, the high-frequency loss becomes profound, and the cut-off frequency gradually spreads to lower frequencies with advancing age (Henry and Chole 1980; Li and Borg 1991). As with human presbycusis, the hearing loss in C57BL/6 mice first appears well after sexual maturity: young mice of this strain have excellent hearing thresholds at all test frequencies. However, in addition to the profound hearing loss at high frequencies in these mice, some studies of C57 also show a secondary hearing loss, less severe in magnitude, at the lowest test frequencies, which also progresses with age (Li and Borg 1991). This low-frequency loss is not characteristic of most forms of human presbycusis (Schuknecht 1974).

The age-related histopathological changes in hair cells and spiral ganglion cells have been well studied in the C57BL/6 mouse (Henry and Chole 1980; Shnerson et al. 1982; Garfinkle and Saunders 1983; Spongr et al. 1997; White et al. 2000). As reported most thoroughly by Spongr et al. (1997), the hair cell loss begins at the cochlear base and gradually spreads apically with advancing age. This lesion includes loss of both inner and outer hair cells, with outer hair cell loss more extensive than inner hair cell loss. Loss of spiral ganglion cells is also seen in the basal turn, consistent with retrograde degeneration occurring secondary to inner hair cell loss (White et al. 2000). The apical

extent of the basal-turn hair cell loss is roughly consistent with the cutoff for high-frequency threshold shifts in these mice (Henry and Chole 1980). However, previous comparisons between histopathology and pathophysiology have noted a poor correlation between the degree/extent of hair cell loss and the pattern of threshold shift (Henry and Chole 1980). In particular, the pattern of hair cell loss does not account for the progressive loss of hearing sensitivity at the low frequencies.

The purpose of the present study was to extend existing descriptions of cochlear histopathology in the aging C57BL/6 mouse to include all structures of the cochlear duct, notably those that have been largely ignored, such as the spiral ligament, spiral limbus, and stria vascularis. From these observations, we hoped to infer (1) which were the functionally important structural changes in the aging C57BL/6 mouse and (2) which changes were primary and which were secondary. To accomplish this, we compared the extent and degree of auditory brain stem response (ABR) threshold shift in an age-graded series of C57BL/6 mice with a thorough quantitative analysis of cochlear histopathology along the cochlear spiral. To accomplish the histopathological analysis, we developed a preparation technique for the mouse cochlea that allows light microscopic evaluation of all structures of the cochlear duct (not just hair cells and spiral ganglion cells) with the cochlear tissue fixed and prepared as if for electron microscopic evaluation, yet assessable first by light microscopy as extra-thick plastic sections.

MATERIALS AND METHODS

Experimental groups and experimental design

Animals used in this study were C57BL/6J or CBA/CaJ mice obtained as young pups from Jackson Laboratories (Bar Harbor, ME) and aged in the animal care facility of the Massachusetts Eye and Ear Infirmary. For each C57BL/6J, a physiological test was scheduled when the animal was either 1.5, 3, 7, or 15 months of age. There were four to five animals in each age group. Recordings of auditory brainstem response (ABR) potentials were obtained from both ears in all but three cases: in one, the animal died before the second side could be evaluated, and, in two others, equipment malfunction prevented recording from the second side. CBA/CaJ mice were tested at either 2.5 months ($n = 4$), 14 months ($n = 1$), or 25 months ($n = 2$). ABRs were obtained from both ears in each of the three older animals. Immediately after the physiological test, each animal was perfused for histological evaluation of any ear for which physiological data were obtained.

Anesthesia and surgical preparation

For physiological testing, mice were anesthetized with xylazine (50 mg/kg i.p.) and ketamine (100 mg/kg i.p.). Surgical preparation involved only making a small slit in the pinna to better visualize the tympanic membrane. Each ear of each animal was tested separately. All procedures were approved by the IACUC of the Massachusetts Eye and Ear Infirmary.

ABR tests

ABR potentials were evoked by acoustic stimulation of each ear and recorded via needle electrodes inserted through the skin (vertex to ipsilateral pinna near tragus with a ground on the back near the tail). Stimuli were 5-ms tone pips (0.5-ms rise–fall with a $\cos^2$ onset envelope, delivered at 40/s). The response was amplified (10,000X), filtered (100 Hz–3 kHz), and averaged with an A–D board in a LabVIEW-driven data acquisition system. Sound level was raised in 5-dB steps from roughly 10 dB below threshold up to 80 dB SPL. At each sound level, 1024 responses were averaged (with stimulus polarity alternated). The software averager included an "artifact reject" feature in which any single response waveform was discarded if the peak-to-peak voltage exceeded 15 μV. ABR "thresholds," defined as the lowest sound level at which the response peaks were clearly present, were read by eye from stacked waveforms obtained at 5-dB sound pressure intervals (up to 80 dB SPL). Thresholds typically corresponded to a level one step below that at which the peak–peak response amplitude began to rise.

Histological preparation

Animals were perfused intracardially with 2.5% glutaraldehyde and 1.5% paraformaldehyde in a 0.065 M phosphate buffer. Both petrous temporal bones were extracted and the round and oval windows were opened to allow intralabyrinthine perfusion of fixative. After overnight postfixation in the same fixative at 4°C, cochleas were osmicated (1% OsO_4 in dH_2O) for 45 min and decalcified (0.1 M EDTA with 0.4% glutaradehyde) for 3 days. After decalcification, cochleas were dehydrated in ethanols and propylene oxide and then embedded in Araldite® resins (Polysciences, Warrenton, PA) and sectioned at 40 μM with a carbide steel knife. Sections were mounted in permount on microscope slides and coverslipped. After light microscopic analysis, sections were floated off slides and remounted for ultrathin sectioning.

Morphometric analysis

For each case, the cochlear spiral was reconstructed in 3-D using Neurolucida® software (MicroBrightField,

Colchester, VT) and tracking the heads of pillar cells as the reference point for cochlear lengths (mean length = 6.53 mm). From these 3-D data, the distance from the base was computed for each section through the duct using custom LabVIEW® software. Next, a standard cytocochleogram was prepared for each ear using high-power oil-immersion objectives and Nomarski optics. In each section, the number of present and absent hair cells was assessed throughout the entire section thickness. Evaluation of both the nuclear and cuticular regions were used to make these assessments. (Other details of the morphometric analysis are given in the relevant figure captions.) Cochlear location was converted into frequency according to frequency map data described by Ehret (1983) which was fit to a mathematical equation: $f\,(\text{kHz}) = 3.109 * (10^{(100-d) * 0.0142}) - 0.7719)$, where d is the percent distance from the cochlear base.

RESULTS

ABR thresholds

Mean ABR thresholds for each of the four age groups are shown in (Figure 1): as absolute thresholds in (Figure 1A) and normalized with respect to those at the youngest age in (Figure 1B). In broad outline, these data are consistent with those reported previously (Li and Borg 1991). In young animals (1.5 and 3.0 months), ABR thresholds in this inbred mouse strain were comparable to the "best" values seen for any of the inbred mouse strains evaluated, including CBA/Ca, which maintains excellent hearing throughout much of its life span (Henry and Chole 1980; Li and Borg 1991). With increasing age, C57BL/6 mice in the present study showed significant high-frequency losses (e.g., at 32 kHz), appearing most dramatically between 3 and 7 months of age and accompanied by low-frequency losses (e.g., at 5.6 kHz) which increased at a slower rate from 1.5 to 15 months. Note that thresholds at 16 kHz remained almost normal until at least 7 months of age and that there was a particularly large variance in the low-frequency thresholds (5.6–16 kHz) in the oldest animal group; a few of the oldest ears retained near-normal hearing in this low-frequency region, whereas others were much more dramatically affected. Interestingly, there were often significant threshold differences between the two ears of a single animal.

Hair cell and neuronal populations

Mean cytocochleograms for the four age groups are shown in (Figures 2A) and (B) for inner and outer hair cells, respectively. The data suggest there are at least two damage foci, one at the cochlear base involving both inner hair cells (IHCs) and outer hair cells (OHCs) and a second in the cochlear apex involving mainly OHCs. The relatively small standard error bars for most groups at most locations indicate that the patterns are quite similar among different members of each age group. In the cochlear base, there was an orderly progression of hair cell loss. With advancing age, the degeneration spread more apically, with OHC loss leading IHC loss along the cochlear spiral. In the cochlear apex, the selective OHC loss was first noticeable at 7 months and rose to almost 40% at 15 months.

These two damage patterns resulted in a hair cell loss profile in the oldest animals that was significantly

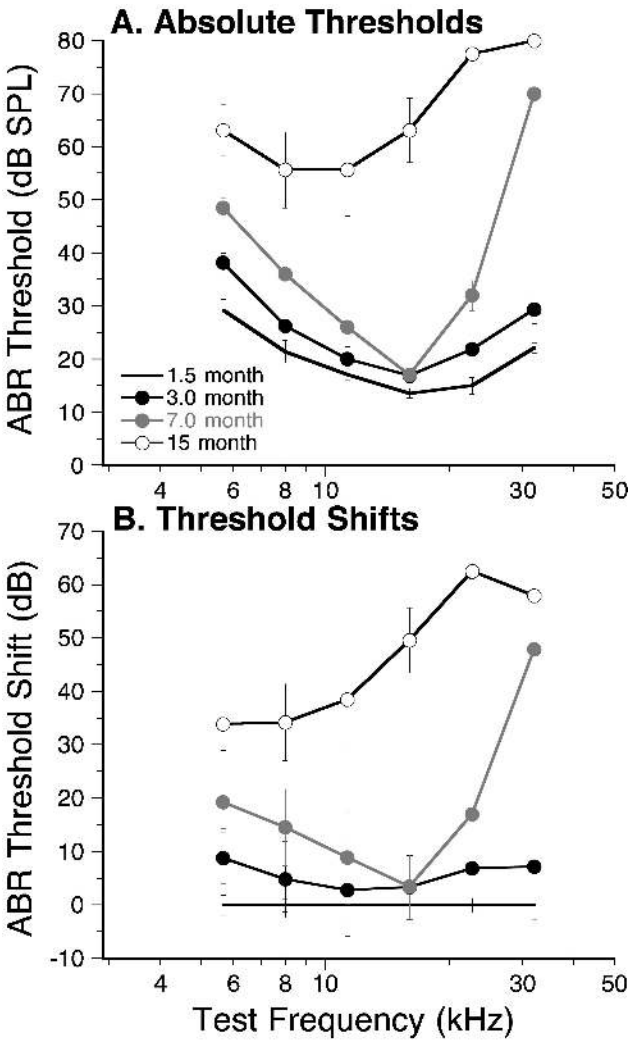

FIG. 1. Average ABR thresholds (+/− SEM) for an age-graded series of C57BL/6 animals. **A** Absolute thresholds, **B** Normalized thresholds with respect to average from the youngest animals. Database for each of the age groups includes (1) 1.5 months=m8 ears from 4 animals; (2) 3.0 months=m7 ears from 4 animals; (3) 7 months=m10 ears from 5 animals; and (4) 15 months=m8 ears from 5 animals.

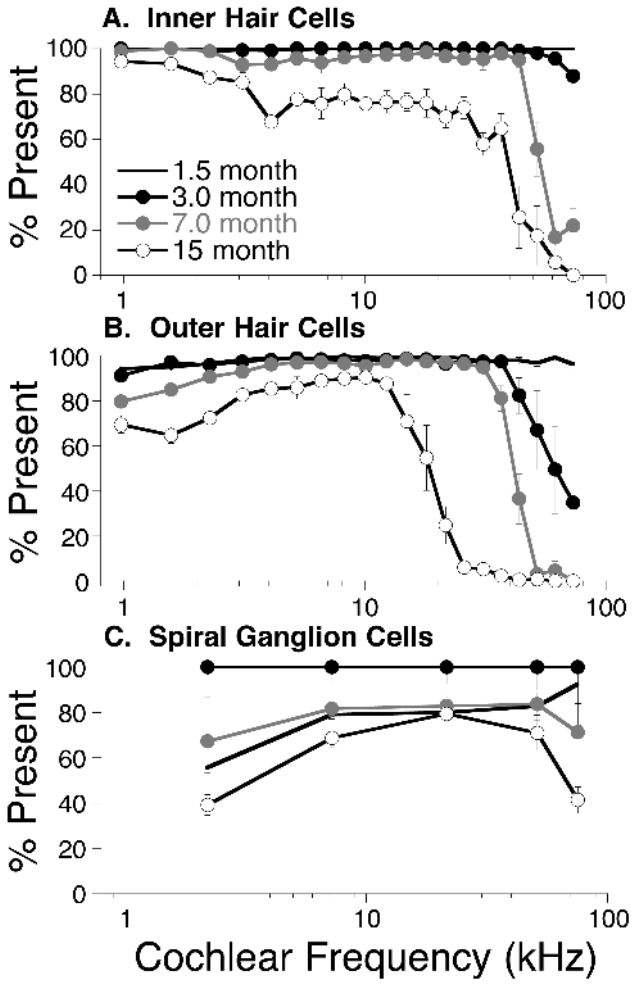

FIG. 2. Average patterns of hair cell loss (**A, B**) and spiral ganglion cell loss (**C**) from the right ears of the same animal database described for (Fig. 1). Error bars indicate standard errors of the mean. The hair cell loss in each case was determined via high-power light microscopic analysis of a complete set of serial sections through each ear. Ganglion cell loss was estimated by sample cell counts in each of 5 cochlear regions in which the ganglion was cut in cross section (1 section in each region from each case). For each cochlear region of each case, a 50-μm by 50-μm mask was applied (through a drawing tube) to a high-power Nomarski view of the center of the ganglion. All neurons within this mask were counted (if and only if a nucleolus were present) at all focal planes throughout the 40-μm thickness of the section. Counts were double-checked and divided by the actual section thickness (read off the calibrated fine focus knob of the microscope). For the graph in **C**, the neuronal densities in each region were normalized to the highest values observed (i.e., those seen at 3 months of age). For all panels, cochlear location is translated into cochlear frequency using a map based on that of Ehret (1983).

different for IHCs than for OHCs. The IHCs showed a monotonically increasing loss from apex to base with a dramatic increase in damage in the extreme base. In contrast, the OHC population remained almost intact in the middle of the cochlea, with damage increasing toward both base and apex, but more rapidly toward the base.

The pattern of spiral ganglion cell degeneration also suggests separate damage foci in the cochlear base vs. apex. As shown in (Figure 2C), neuronal densities were measured at 5 cochlear locations in each animal from each age group. In the oldest age group, the mean data show significant neuronal degeneration in both the extreme base and apex (more than 60% loss with respect to the 3-month-old animals.[a]

The basal-turn neuronal loss seen among the 15-month animals is expected from, and spatially consistent with, a secondary retrograde degeneration due to the basal-turn loss of IHCs. In contrast, the equally severe apical neuronal loss at 15 months appears to be primary degeneration, in the sense that the IHCs are largely intact in the extreme apex.

Another striking difference in the neuronal pathologies between the cochlear base and apex is the presence of numerous multicellular somatic aggregates of spiral ganglion cells in which all constituents appear to have lost their myelin sheaths. Such aggregates were restricted to the apical half of the cochlea. As shown in (Figure 3A), these clumps can range in size from clusters of 3–5 cells to large cystlike formations of tens of cells. Such neuronal cysts have not been observed in other murine cochleas, including CBA/CaJ, 129/SvEv, and FVB/N, at any age (Liberman, unpublished observations). Some of these large cysts appear to have hollow (fluid-filled) centers. The total aggregate size of these cyst formations changed little from 1.5 through 7 months of age; however, there was a significant rise in their overall prevalence in the 15-month animals (Fig. 3B).

Tectorial membrane, stria vascularis and spiral ligament

"Accessory" structures of the cochlear duct were examined in all ears, at all ages, for signs of histopathology. Structures systematically assessed included spiral limbus, spiral ligament, stria vascularis, and tectorial membrane. Of these structures, the initial qualitative examination suggested significant and systematic age-related changes in all of them, except in the spiral limbus. Thus, for each of the latter three structures, a method was devised for quantification of the suspected changes in each region.

For the tectorial membrane, the striking change was a systematic decrease in cross-sectional area with age, as can be seen in the photomicrographs in (Figure 4) taken from identical cochlear locations in a 1.5-

[a] The apparent rise in neuronal counts from the 1.5-month to the 3.0-month groups suggests a significant postnatal proliferation of spiral ganglion cells (given that the total cross-sectional area of the ganglion also increased slightly from the 1.5- to the 3.0-month time point). However, mitotic figures were never observed.

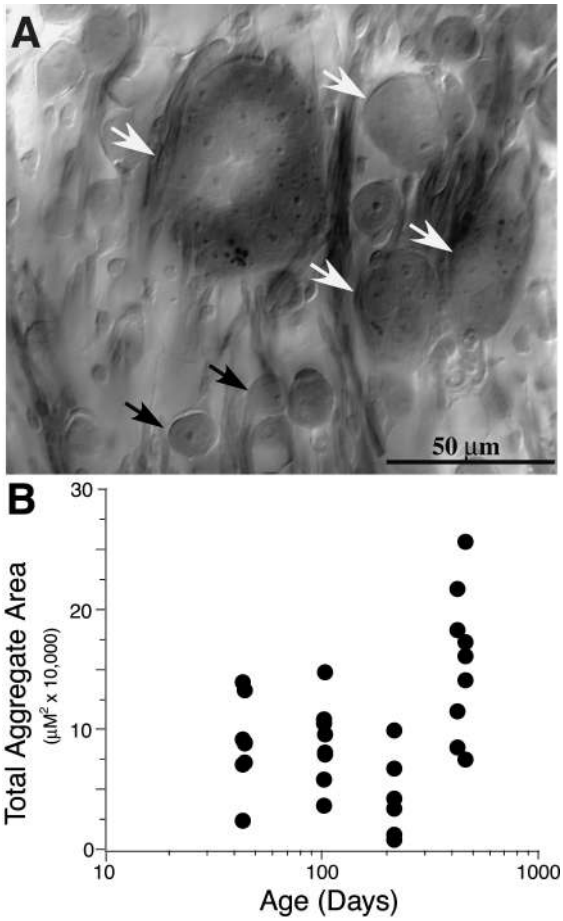

FIG. 3. **A.** Photomicrograph of the somatic aggregates (open arrows) seen in the spiral ganglion of C57BL/6 mice of all ages. Some of the normal-looking, nonaggregated spiral ganglion cells are indicated by the filled arrows. **B.** Total area of somatic aggregates in each of the ears analyzed. Each filled circle represents a different cochlea. In each cochlea, the silhouette (i.e., maximum) area of each of the somatic aggregates was digitized. The area of each aggregate was computed, and these values were summed across all sections. Such aggregates were seen only in the apical half of the cochlea.

and a 15-month-old animal. To quantify this, the cross-sectional area was measured in each ear from each age group at two cochlear locations. As shown in (Figure 5A), there were systematic decreases in tectorial membrane size at both the 2- and the 21-kHz regions. These regions were chosen because, given our sectioning angle, they were cut in an almost perfect cross section. The same trend toward decreased size with increasing age appeared to hold true throughout the cochlea; however, detailed measurements were not made.

Qualitative evaluation suggested that the stria vascularis became increasingly thin with increasing age. To examine this possibility more quantitatively, the average width of the stria was measured in each ear at 5 cochlear regions (at exactly the midpoint of each cochlear half-turn to produce consistent cross sections of the stria). As shown in (Figure 5B), the qualitative impression was substantiated by the measurements: the average strial width decreased systematically with age in every cochlear location assessed, although the percentage changes were smallest in the-21 kHz region.

The most striking histopathology outside the organ of Corti was seen in the spiral ligament, where clear-cut loss of cells was evident, especially among the type IV fibrocytes. The cells making up the mammalian spiral ligament include four classes of fibrocytes as well as the long basal processes of the root cells, whose apical surfaces reach to the endolymphatic space in the region of the outer sulcus. The different types of fibrocytes, classified on the basis of their size, shape, orientation, and cytochemistry (Spicer and Schulte 1991), tend to cluster in reasonably well-defined portions of the spiral ligament, as illustrated in (Figure 6). Even a cursory analysis revealed significant and systematic loss of fibrocytes in the spiral ligament with advancing age. As illustrated by the micrographs in (Figures 4C) and (D), cell loss was most severe in the region where the basilar membrane joins the spiral ligament, i.e., in the region of the type IV fibrocytes.

Our qualitative analysis suggested that, in any one cochlear region, cell loss was always first noticeable among the type IV fibrocytes. With increasing age, or with increasing proximity to the basal and apical extremes, the damage spread to include loss of type II fibrocytes. Type I fibrocytes were often depopulated in the older animals, especially in the region between the stria vascularis and the capsular bone, and especially in the upper basal turn and the extreme apex. On the other hand, clear-cut loss of type III fibrocytes was never seen in any age group.

To document these apparent trends in more quantitative fashion, a rating scale was devised in which the average cell loss in each fibrocyte class was estimated for each section through the ligament in every ear in the study. Loss was estimated as either 0 ("normal"), 1/3, 2/3, or 3/3 (complete loss). For this analysis, "normal" was defined as the highest cell density in any of the ears analyzed, which, for all cochlear regions, was found in two cochleas from the youngest animals. As described below, these high densities were comparable to those seen in other murine strains. After this semiquantitative analysis, explicit cell counts were made in a number of randomly sampled regions for the type IV fibrocytes, and the general accuracy of these visual estimates was verified (data not shown). Mean data for estimated fibrocyte loss for each of the four age groups are shown in (Figure 7). Note that (1) significant loss of type IV fibrocytes was visible in the apical turn at even the youngest age; (2) with advancing age the type IV loss worsened in both the apical and basal halves of the cochlea, with relative

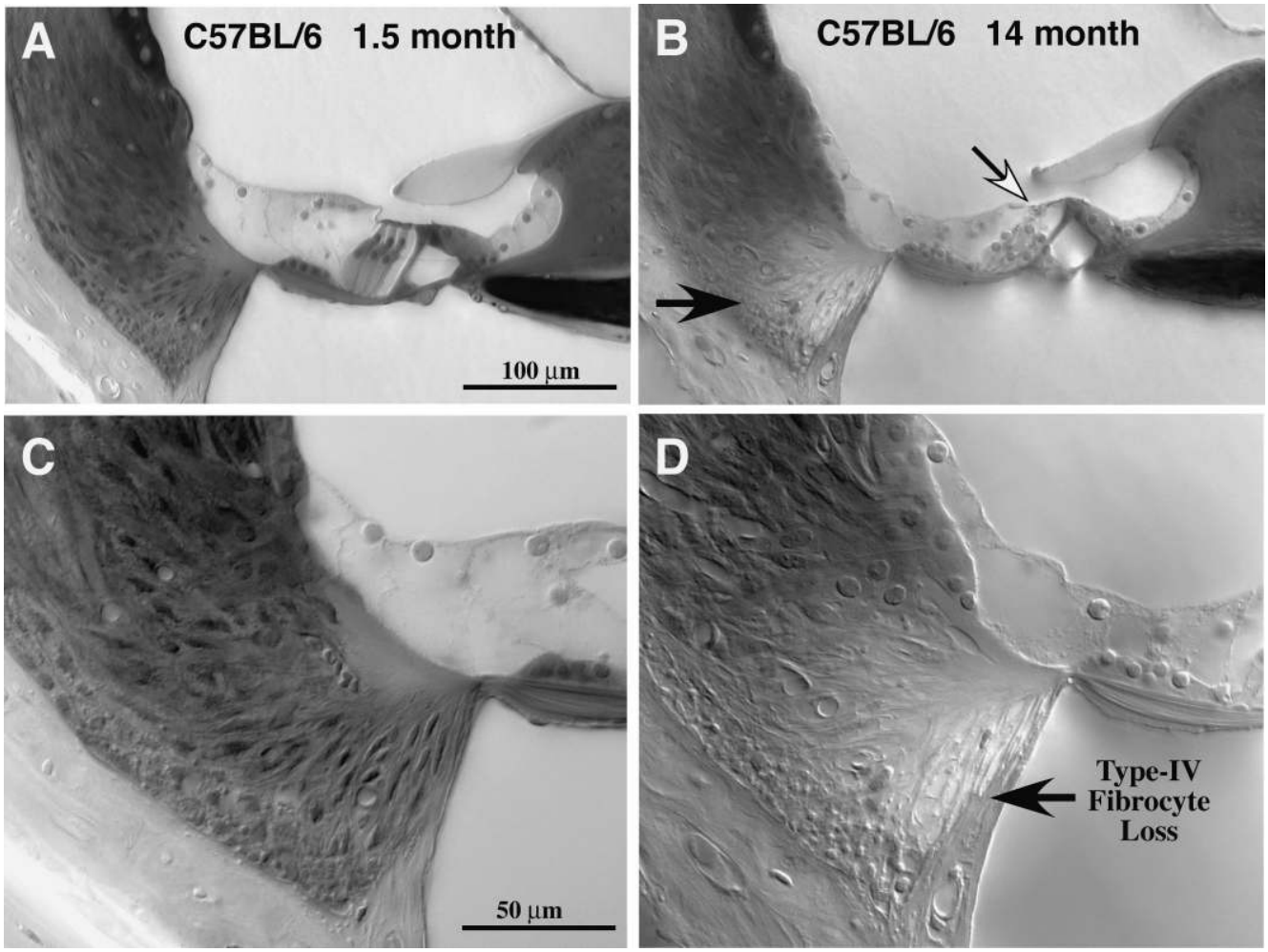

FIG. 4. Photomicrographs of the cochlear duct in upper basal turn of a young (1.5 months) C57BL/6 mouse (**A**) and an older (15 months) mouse (**B**). The older ear shows loss of OHCs (unfilled arrow) and loss of the type IV fibrocytes (filled arrow). The apparent shrinkage of the tectorial membrane is also visible. **C** and **D** Same sections as in **A** and **B** but at higher magnification to highlight the loss of type IV fibrocytes. Scale bars **A** and **C** apply to **B** and **D**, respectively.

sparing of the 30–40-kHz region (especially at 3 months of age) (3) loss of type II fibrocytes was much less severe, with loss largely restricted to the extreme base in only the oldest animals; and (4) loss of type I fibrocytes was worst in the extreme apex and in a region of the upper basal turn corresponding to the 20-kHz region.

To determine if fibrocyte pathology is a universal correlate of aging in the murine cochlea, regardless of the degree of age-related hearing loss, a small group of aged CBA/CaJ cochleas was evaluated both histologically and physiologically. As seen in (Figure 8A) and reported by others (Li and Borg 1991), the ABR thresholds in this strain change little in the first year of life and show only slight elevation at all test frequencies by 2 years of age. As illustrated by the micrographs in Figures 8B and (C), the spiral ligament, as well as hair cell populations, in CBA/CaJ remains essentially normal, even at 25 months of age.

DISCUSSION

Patterns of hair cell and neuronal loss: comparisons to previous studies

Almost all previous studies of the morphological correlates of age-related hearing loss in the C57BL/6 cochlea have focused on the hair cells and/or spiral ganglion neurons. Previous studies of hair cells have noted the predominant basal-to-apical gradient in hair cell loss with advancing age, and all the present data on hair cell and neuronal loss patterns are qualitatively consistent with this earlier literature (e.g., Henry and Chole 1980; Spongr et al. 1997) and are also similar to those reported for another inbred mouse strain (BALB/c) with progressive hearing loss (Willott et al. 1998).

The mean cytocochleograms from the present study reveal a complex pattern of hair cell loss indicating

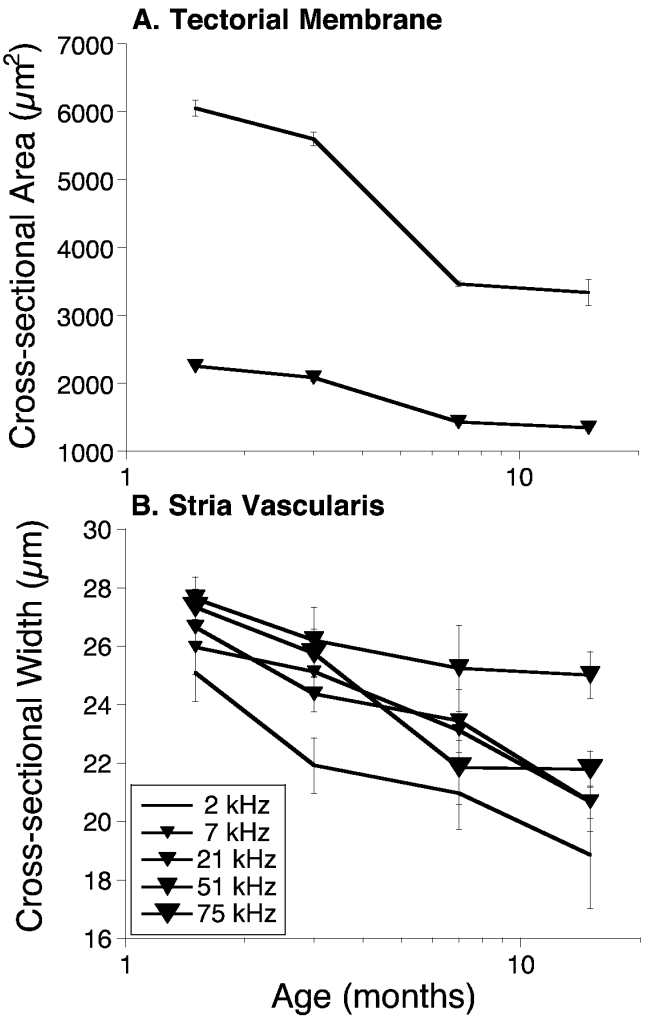

FIG. 5. Age-related changes are seen in the cross-sectional area of the tectorial membrane (**A**) and the stria vascularis (**B**) in the C57BL/6 mouse. Average values (+/− SEM) were determined for four cochlear locations from the right ear of every animal in this study. For each region in each ear, the section representing the truest cross section through the cochlear duct was selected for measurement. Measurements were made via computerized planimetry with a 20× or 40× objective. For the tectorial membrane, the outline was traced and the cross-sectional area determined. For the stria vascularis, the outline was traced and this cross-sectional area was divided by the "height" of the stria, i.e., the length of an imaginary line running through the intermediate cells, to compute an average "width" of the organ.

more than one underlying degenerative process. Only one previous study provided such detailed data as a function of age in C57BL/6 (Spongr et al. 1997). Although the ages examined in that study (1, 3, 8, 18, and 26 months) were different from those studied here (1.5, 3, 7,and 15 months), there are a number of quantitative similarities between the results. Both studies document the region of total hair cell loss in the basal turn, which moves progressively more apically with advancing age (OHC loss leading IHC loss along the spiral). In addition to this abrupt hair cell gradient [reminiscent of the lesion pattern following ototoxic drugs (Dallos and Wang 1974; Kiang et al. 1976)], both studies also show a gradient of significant—but subtotal—IHC loss seen throughout almost the entire cochlea in the older animals (Fig. 2A). This gradual apical–basal gradient of subtotal IHC loss is not seen following ototoxic drug damage (Dallos and Wang 1974; Kiang et al. 1976) and is not paralleled by a loss of OHCs. Indeed, the gradient of OHC loss is in the opposite direction (increasing toward the apex). This increasing OHC loss in apical turns of older animals (Fig. 2B) is not evident in the previous quantitative study, however, data in the latter are averaged over larger distance bins and such a trend might be difficult to resolve.

The patterns of neuronal loss are also complex (Fig. 2C) and suggestive of separate damage foci in the base and the apex of the cochlea. The neuronal loss in the basal turn is consistent with the well-studied cochlear phenomenon of secondary neuronal degeneration subsequent to IHC loss seen after acoustic injury as well as ototoxic drug lesions (Spoendlin 1984, Kiang et al. 1976; Liberman and Kiang 1978). Given that 90%–95% of all spiral ganglion neurons contact only IHCs (Spoendlin 1969), the fate of the OHCs is not as critical to the survival of most cochlear afferent neurons. A previous quantitative study of ganglion cell loss in the base (White et al. 2000) similarly concluded that neuronal loss was secondary to loss of IHCs and progressed in retrograde fashion, with loss of distal axon (within the osseous spiral lamina) occurring before loss of cell body (in the spiral ganglion).

Comparison of hair cell and neuronal loss patterns (Fig. 2) suggests that the neuronal loss in the apical cochlea is a primary degeneration. It is certainly not occurring secondary to IHC loss given that the IHC population is steadily increasing from the midcochlear regions towards the apex, whereas the ganglion cell population is steadily declining. Although the latter gradient is mirrored in the OHC loss gradient, it is unlikely that the OHC loss is directly responsible for the neuronal loss: (1) as noted above, the afferent innervation of OHCs is exclusively via type I SGCs which constitute only 5% of the cochlear afferents and (2) correspondingly, OHC loss *per se* (via ototoxic drugs or acoustic injury) does not appear to cause significant neuronal degeneration (Kiang et al. 1976).

Another line of evidence suggesting that the neuronal degeneration in the apex is fundamentally different from that in the base is the presence of somatic clumping in the spiral ganglion (Fig. 3). This phenomenon has been previously described in a combined light and electron microscopic study of the cochlear afferents in C57BL/6 (Cohen et al. 1990) but has not

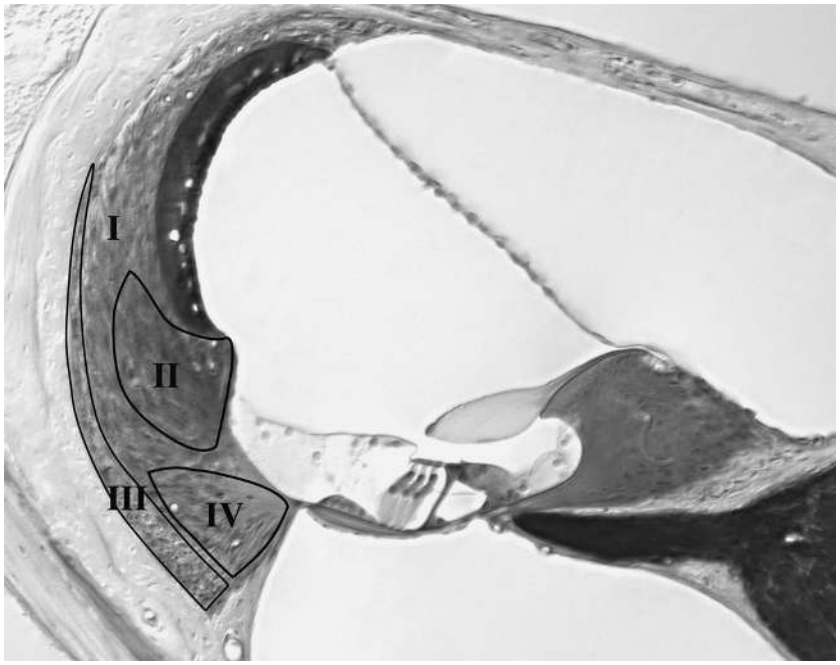

FIG. 6. Photomicrograph of the cochlear duct indicating the approximate locations of the type I, II, III, and IV fibrocytes in the basal turn of the mouse cochlea, according to previous studies (Spicer and Schulte 1991). Areas in which type II, III, and IV cells are found are indicated by the labeled contours. Type I fibrocytes can be found throughout the rest of the spiral ligament, not enclosed by contours.

been described in any other type of cochlear pathology, nor in cochleas from any other mouse strain. As reported in the previous electron-microscopic study, this clumping of neuronal cell bodies is associated with a generalized loss of myelin ensheathment of the cochlear neurons. In the present study, we documented that this phenomenon, although present in the youngest animals, was seen exclusively in the apical half of the cochlea and clearly increased in prevalence with advancing age.

Fibrocyte pathology in the C57BL/6 mouse

A large body of recent ultrastructural and immunohistochemical work has suggested that the function of the mammalian spiral ligament is not simply the mechanical suspension of the basilar membrane implicit in the name chosen by early anatomists (Spicer and Schulte 1991; 1996; Kikuchi et al. 1995). The rich array of membrane transporters present in the spiral ligament fibrocytes and the gap junctional linkages among and between cell groups in the ligament (and between the ligament and the stria vascularis) have suggested that an important function of the spiral ligament is to transport K^+ ions (shuttled across the hair cells during transduction) from the organ of Corti back to the stria vascularis to be pumped back into scala media (Spicer and Schulte 1996). Furthermore, previous work in the gerbil has implicated degeneration in the spiral ligament as an important contributing factor to age-related hearing loss in that animal model (Schulte and Schmiedt 1992; Spicer et al. 1997).

A recent immunohistochemical study by Ichimaya et al. (2000) has suggesed that alterations in the cochlear lateral wall (i.e., spiral ligament, spiral prominence, and/or stria vascularis) might contribute to the age-related hearing loss in C57BL/6. Although they failed to find any clear-cut histopathology in conventional hematoxyolin-eosin stained sections, they reported progressively reduced immunostaining for connexin 26, a protein involved in the formation of gap junctions, in the spiral ligament of 6-week vs. 6-month vs. 12-month old mice. This decrease in connexin immunoreactivity was associated with increases in Na, K–ATPase immunostaining in both the spiral ligament and the stria vascularis. Their observations, particularly the decrease in connexin staining, are consistent with the present results showing clear-cut degeneration of several classes of spiral ligament fibrocytes in the aging C57BL/6 cochlea. It is not clear why the clear-cut cellular loss we document was not visible/present in the material examined by Ichimaya et al. (2000); however, it may be hard to assess fibrocyte loss when the sections are thinner than the 40 μm thickness used here (given their relatively low density even in normal ears).

The present study provides clear evidence for significant and widespread degeneration in the spiral ligament in the aging C57BL/6 mouse. This degeneration was particularly prevalent among the type IV fibrocytes located in a triangular region just inferior to the point of insertion of the basilar membrane (Fig. 6), a region which has also been called the "basilar crest." According to histochemical studies, these fibrocytes are rich in carbonic anhydrase as well as Na, K–ATPase (Spicer and Schulte 1991) and are thus implicated in

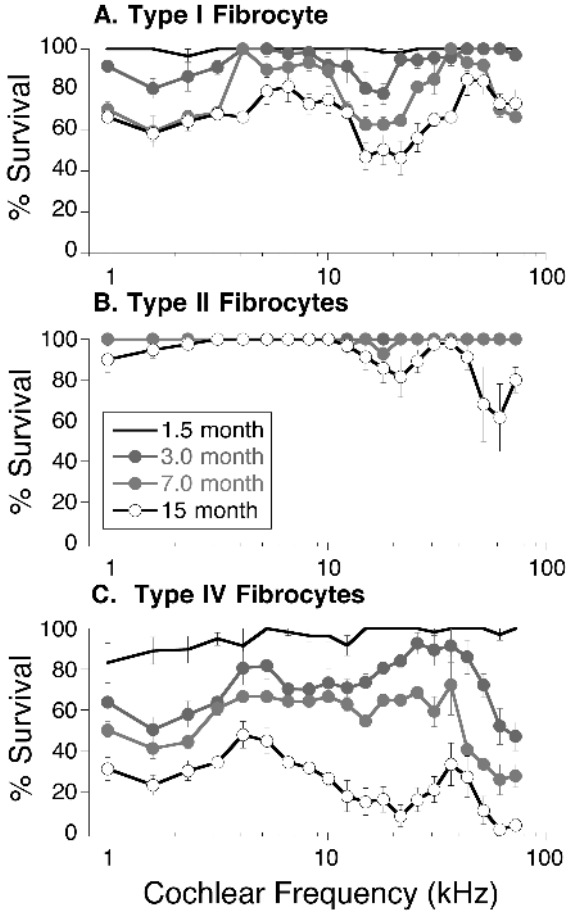

FIG. 7. **A–C** Mean survival of three classes of fibrocytes as a function of cochlear location in the different age groups of C57BL/6 mice. Right ears from all animals were assessed. Error bars indicate +/− SEM. Cell survival was assessed in semiquantitative fashion. An observer blind to the physiological data for each case estimated, in every section through the cochlear duct, the percentage of fibrocytes remaining: grade 0, 0%–25% remaining; grade 1, 25%–50%; grade 2, 50%–75%; grade 3, 75%–100%. For final plotting, this 0–3 grading scale was converted to a 0%–100% survival index. These estimates of cell loss were based on cell nuclei and were referred to the maximum density seen in any of the ears assessed (found in two of the four youngest cochleas). Care was taken to assess each cochlear region separately because the detailed appearance of the spiral ligament changes dramatically from base to apex in all murine strains we examined: CBA/CaJ, C57BL/6J, 129/SvEv, and FVB/N. Before the final analysis, the test–retest reliability of the same observer was evaluated as well as the agreement between two different observers. The final analysis of all ears was performed in a concentrated fashion over consecutive days to minimize criterion drift.

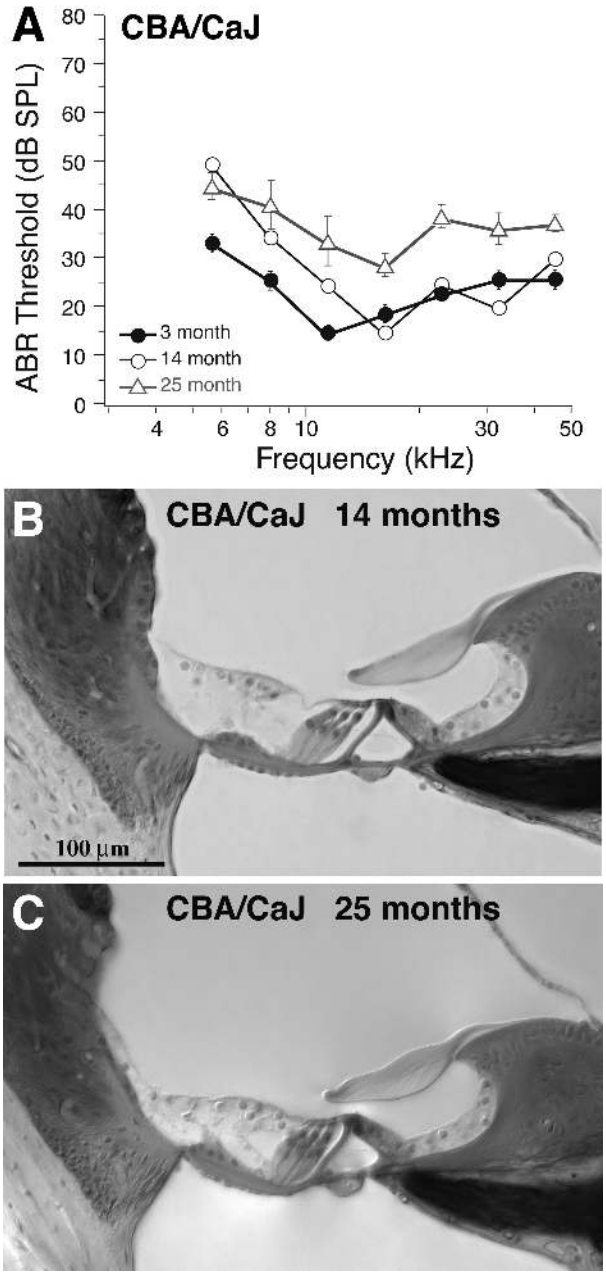

FIG. 8. Pathophysiology and histopathology in the aging CBA/CaJ mouse shows that, despite slight threshold elevations at ages >14 months (**A**), the spiral ligament in this strain does not show fibrocyte degeneration. Photomicrographs **B** and **C** are from the upper basal turn of a 14-month-old and a 25-month-old animal, respectively. Scale bar in **B** also applies to **C**.

ion homeostasis in the cochlear duct. A recent *in situ* hybridization study of a receptor tyrosine kinase (EphA4) clearly shows a highly selective and concentrated expression of this receptor in the type IV fibrocytes of the mouse ear (van Heumen et al. 2000), lending credence to the idea that this particular region of the ligament contains a functionally distinct cell class.

The present data suggest the possibility that degeneration in the spiral ligament, particularly among the type IV fibrocytes, may be an important locus of primary cochlear pathology in the C57BL/6 strain and that changes in the lateral wall may be the root cause of the age-related hearing loss, or at least a very early step in the degenerative process. The major argument in favor of this view is the quantitative histopathological analysis documenting that the type IV degeneration leads the loss of hair cells and neurons in both space

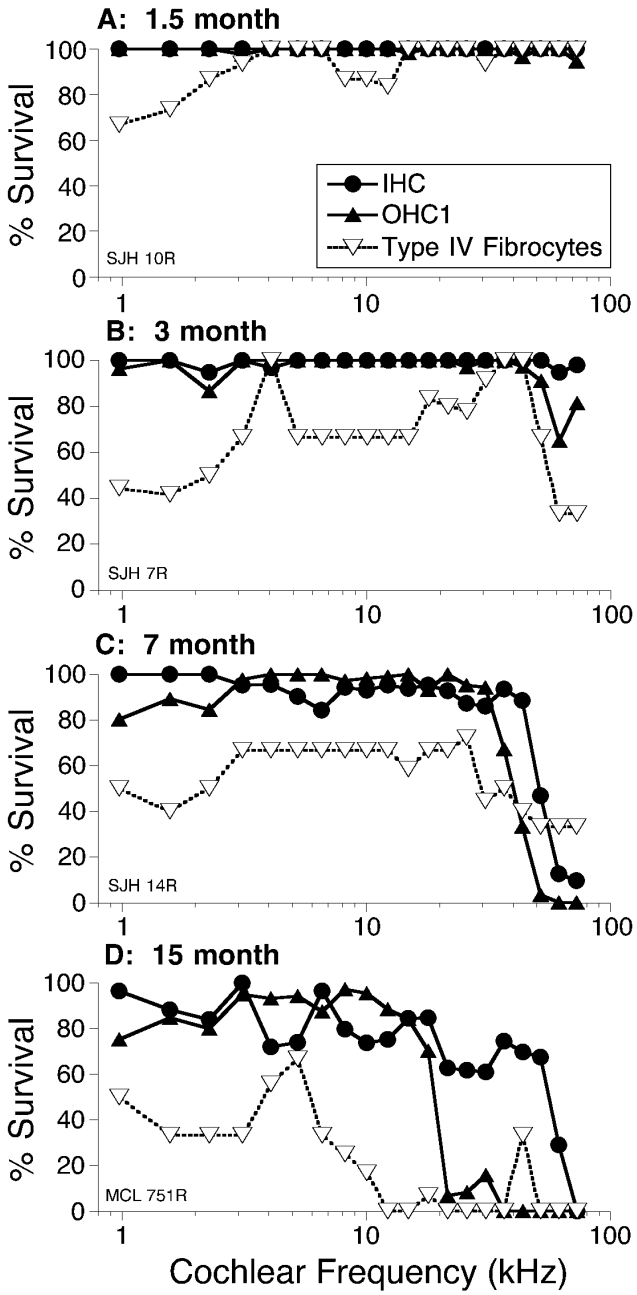

FIG. 9. A–D Comparison of the patterns of hair cell and type IV fibrocyte degeneration in 4 representative cases, one from each of the four age groups. Hair cell and fibrocyte analysis were carried out as described for Figs. 2 and 7, respectively.

and time. First, in all ears with a basal region of total OHC loss (Fig. 9), there was an overlapping region of severe type IV cell loss which, in each case, extended further apically than the OHC loss. Thus, the apically advancing front of severe type IV degeneration leads the advancing front of severe hair cell loss along the cochlear spiral. Second, for animals 7 months or younger, there was significant loss of spiral ligament fibrocytes throughout the apical half of the cochlea without concomitant loss of hair cells (compare mean data in (Figs. 2 and 7).

Thus, if one considers a single cochlear location, the age of onset of significant degeneration in spiral ligament fibrocytes predates the appearance of significant hair cell loss. The age of onset for a variety of cochlear structures in C57BL/6 can be compared more explicitly in (Figure 10). In this plot, we consider two cochlear regions, the part of the upper basal turn, tuned to about 21 kHz, and the middle of the second turn, tuned to roughly 7 kHz, according to the cochlear frequency map for the mouse (Ehret 1983). In both these cochlear regions, there is virtually no hair cell loss until after 7 months of age, yet there is clear-cut change in the mean survival of type IV fibrocytes evident by three months of age.

Fibrocyte pathology as a primary cause of age-related hearing loss

The availability of ABR data on the same animals examined histopathologically in the present study allows inferences to be made as to which types of structural change may be functionally significant in this animal model of age-related hearing loss.

Comparison of the data in (Figure 10) suggests that the progression of fibrocyte loss with age mirrors the loss of ABR thresholds with age. Put another way, the threshold shift in the 7- or 21-kHz regions seen at ages $\leq$ 7 months cannot be explained by a loss of hair cells (there is virtually none). Although submicroscopic damage to remaining hair cells (or other structures) cannot, of course, be ruled out, the threshold shift may arise primarily from reduction in the endolymphatic potential resulting from the loss of type IV fibrocytes (see below).

Similarly, if one considers the overall progression of ABR thresholds with age and the overall patterns of hair cell loss with age, one concludes that although the precipitous rise in ABR thresholds at the highest frequencies ($>$ 20 kHz) may be explained largely by the total loss of hair cells in the basal turn, the accumulating threshold elevations at lower frequencies ($<$ 20 kHz) are not well explained by the overall pattern and degree of hair cell loss in more apical regions (compare data in (Figs. (1) and (2)). Some or all of this functional deficit may arise from pathology in the fibrocytes of the lateral wall.

The neuronal pathology seen throughout the apical half of the cochlea may also contribute to the low-frequency hearing loss. However, several arguments suggest that contribution may be minimal. First, the somatic aggregation in the ganglion was present at the youngest age examined (when thresholds were normal) and its prevalence did not increase for the first 7 months (although low-frequency thresholds

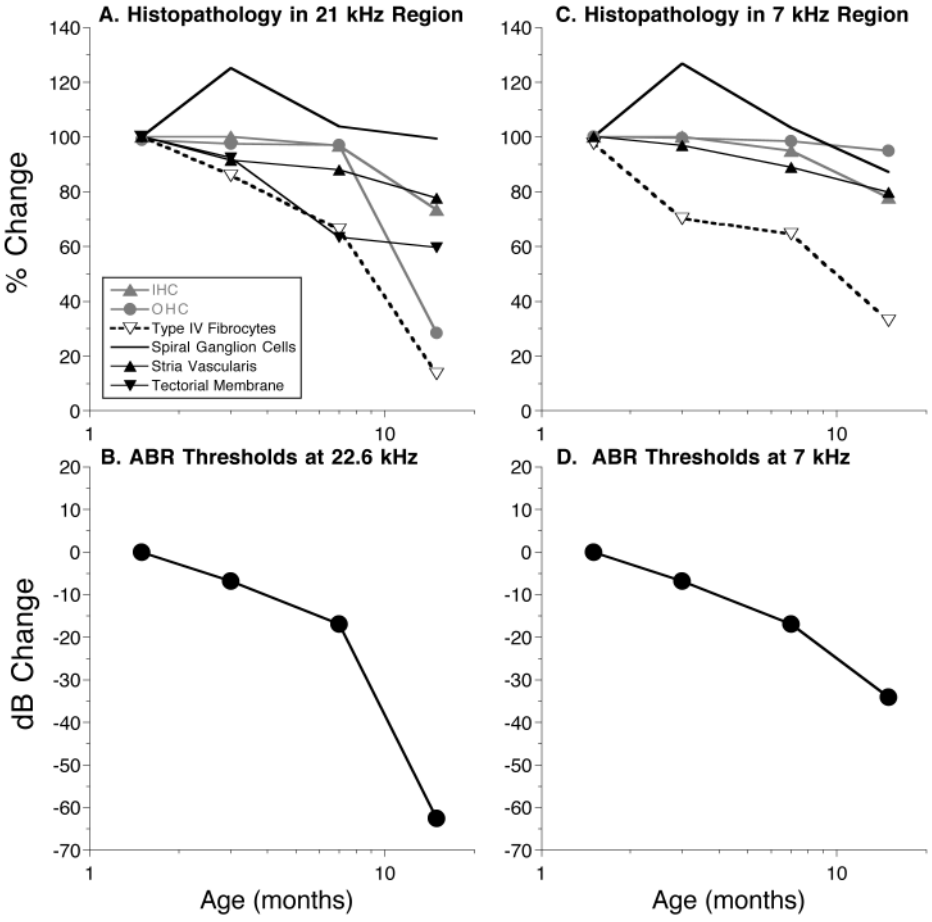

FIG. 10. The age-related changes in cochlear structures seen in the upper basal turn (**A**) or second turn (**C**) compared with the age-related threshold shift at the test frequencies appropriate for each region (**B** and **D**, respectively). Data in **A** and **C** are replotted from histopathological data of hair cells and ganglion cells from Fig. 2, stria and tectorial membrane from Fig. 5, and type IV fibrocytes from Fig. 7.

were rising). Second, other animal models of neuronal degeneration show that, if outer hair cell function remains normal, the loss of functional neurons needs to be much greater than 50% before significant impact is seen on gross evoked neural potentials such as ABR or CAP (Liberman et al. 1997).

Combining the present histopathological data for the C57BL/6 strain with recent speculations as to the function of fibrocytes in the lateral wall, the following hypothesis for the etiology of the AHL in this mouse can be advanced. The genetic deficit in the C57BL/6 strain may cause early-onset degeneration of the type IV fibrocytes. In this context, it may be significant that a mutation in the *brn4* gene has been suggested to cause selective degeneration of the spiral ligament fibrocytes in the mouse (Minowa et al. 1999). As these fibrocytes disappear, ion homeostasis in the cochlea may be disrupted (perhaps, in particular, K^+ recycling to the stria vascularis), leading to chronically decreased endolymphatic potential (EP). An EP drop would immediately lead to threshold elevations in the affected regions (Sewell 1984). Furthermore, chronic changes in EP could lead to alterations in endolymph ion composition due to the changes in constraints on ion content imposed by the standing potential. Such putative abnormalities in local endolymph ion composition might lead ultimately to hair cell degeneration and might also underlie the observed changes in tectorial membrane size (Fig. 5A). Given an estimated electrical length constant of ~2 mm for scala media (Johnstone et al. 1966), lateral wall dysfunction in the cochlear base would not be expected to affect hair cells in the cochlear apex.

The best evidence for hair cell loss occurring secondary to endolymph abnormalities is from other murine deafness models, where the hair cells degenerate subsequent to changes in strial function due to failure of melanocyte migration (Steel and Barkway 1989; Cable et al. 1992). Once the hair cells degenerate, the neuronal degeneration will follow, as in many other forms of sensorineural hearing loss. One key test of this view would be to measure the EP in an age-graded series of C57BL/6 mice. According to our literature searches, EP data have never been published for the aging C57BL/6 mouse.

Atrophy of the spiral ligament has also been reported in aging human temporal bones. According to Wright and Schuknecht (1972), patchy loss of ligament fibrocytes is seen in aging human ears without any significant history of hearing loss. Interestingly,

that cellular loss appeared first in the "basilar crest" region of the ligament, which corresponds to the type IV fibrocyte region described here. In their study of 151 human temporal bones, Wright and Schuknecht also identified 15 cases with high-frequency hearing loss due to aging in which there was severe atrophy of the spiral ligament, especially in the basal turn. They hypothesized that this type of pathology would lead to hearing loss by changing cochlear mechanics (cochlear conductive type of presbycusis), rather than via an important ionic role as hypothesized here. Nevertheless, it appears likely that spiral ligament pathology is part of the etiology in some subset of human AHL cases.

ACKNOWLEDGMENTS

This work was supported by a grant from the NIDCD: RO1 DC0188.

REFERENCES

CABLE J, BARKWAY C, STEEL KP. Characteristics of stria vascularis melanocytes of viable dominant spotting (Wv/Wv) mouse mutants. Hear. Res. 64:60–20, 1992.

COHEN GM, PARK JC, GRASSO JS. Comparison of demyelination and neural degeneration in spiral and Scarpa's ganglion of C57BL/6 mice. J. Electron Microsc. Tech. 15(2):165–172, 1990.

DALLOS P, WANG C-Y. Bioelectric correlates of kanamycin intoxication. Audiology 13:277–289, 1974.

EHRET G. Peripheral anatomy and physiology II. In: Willott JF, (ed) The Auditory Psychobiology of the Mouse. Charles C. Thomas Springfield, IL 169–200, 1983.

GARFINKLE TJ, SAUNDERS JC. Morphology of inner hair cell stereocilia in C57/6J mice as studied by scanning electron microscopy. Otolaryngol. Head Neck Surg. 91(4):421–426, 1983.

HENRY K, CHOLE R. Genotypic differences in behavioral, physiological and anatomical expression of age-related hearing loss in the laboratory mouse. Audiology 19:369–383, 1980.

ICHIMAYA I, SUZUKI M, MOGI G. Age-related changes in the murine cochlear lateral wall. Hear. Res. 139:116–122, 2000.

JOHNSTONE BM, JOHNSTONE JR, PUGSLEY LD. Membrane resistance in endolymphatic walls of the first turn of the guinea pig cochlea. J. Acoust Soc. Am. 40:13998–14004, 1966.

KIANG NYS, LIBERMAN MC, LEVINE RA. Auditory-nerve activity in cats exposed to ototoxic drugs and high-intensity sounds. Ann. Otol. Rhinol. Laryngol. 85:752–768, 1976.

KIKUCHI T, KIMURA RS, PAUL DL, ADAMS JC. Gap junctions in the rat cochlea: immunhistochemical and ultrastructural analysis. Anat. Embryol. 191:101–118, 1995.

LI HS, BORG E. Age-related loss of auditory sensitivity in two mouse genotypes. Acta Otolaryngol. (Stockh.) 111:827–834, 1991.

LIBERMAN MC, CHESNEY CP, KUJAWA SG. Effects of selective inner hair cell loss on DPOAE and CAP in carboplatin-treated chinchillas. Aud. Neurosci. 3:255–268, 1997.

LIBERMAN MC, KIANG NYS. Acoustic trauma in cats, cochlear pathology and auditory-nerve activity. Acta Otolaryngol. 358:5–63, 1978.

MINOWA O, IKEDA K, SUGITANI Y, OSHIMA T, NAKAI S, KATORI Y, SUZUKI M, FURUKAWA M, KAWASE T. Altered cochlear fibrocytes in a mouse model of DFN3 nonsyndromic deafness. Science 285:1363–1364, 1999.

SCHUKNECHT HF. Pathology of the Ear. Harvard University Press, Cambridge, MA, 1974.

SCHULTE BA, SCHMIEDT RA. Lateral wall Na,K–ATPase and endocochlear potentials decline with age in quiet-reared gerbils. Hear. Res. 61(1):35–46, 1992.

SEWELL WF. The effects of furosemide on the endocochlear potential and auditory-nerve fiber tuning curves in cats. Hear. Res. 14:305–314, 1984.

SHNERSON A, DEVIGNE C, PUJOL R. Age-related changes in the C57BL/6J mouse cochlea. II. Ultrastructural findings. Dev. Brain Res. 2:77–88, 1982.

SPICER SS, GRATTON MA, SCHULTE BA. Expression patterns of ion transport enzymes in spiral ligament fibrocytes change in relation to strial atrophy in the aged gerbil cochlea. Hear. Res. 111:93–102, 1997.

SPICER SS, SCHULTE BA. Differentiation of inner ear fibrocytes according to their ion transport related activities. Hear. Res. 56:53–64, 1991.

SPICER SS, SCHULTE BA. The fine structure of spiral ligament cells relates to ion return to the stria and varies with place-frequency. Hear. Res. 100:80–100, 1996.

SPOENDLIN HH. Innervation of the organ of Corti of the cat. Acta Otolaryngol. (Stockh.) 67:239–254, 1969.

SPOENDLIN HH. Factors inducing retrograde degeneration of the cochlear nerve. Ann. Otol. Rhinol. Laryngol. Suppl. 112 93:76–82, 1984.

SPONGR VP, FLOOD DG, FRISINA RD, SALVI RJ. Quantitative measures of hair cell loss in CBA and C57BL/6 mice throughout their life spans. J. Acoust. Soc. Am. 101:3546–3553, 1997.

STEEL KP, BARKWAY C. Another role for melanocytes: their importance for normal stria vascularis development in the mammalian inner ear. Development 107:453–463, 1989.

VAN HEUMEN WRA, CLAXTON C, PICKLES JO. Expression of EphA4 in developing ears of the mouse and guinea pig. Hear. Res. 139:42–50, 2000.

WHITE JA, BURGESS BJ, HALL RD, NADOL JB. Pattern of degeneration of the spiral ganglion cell and its processes in the C57BL/6J mouse. Hear. Res. 141:12–18, 2000.

WILLOTT JF, TURNER JG, CARLSON S, DING D, BROSS LS, FALLS WA. The BALB/c mouse as an animal model for progressive sensorineural hearing loss. Hear. Res. 115:162–174, 1998.

WRIGHT JL, SCHUKNECHT HF. Atrophy of the spiral ligament Arch. Otolaryngol. 96:16–21, 1972.